Differential AKT dependency displayed by mouse models of $BRAF^{V600E}$-initiated melanoma

Victoria Marsh Durban,[1] Marian M. Deuker,[1] Marcus W. Bosenberg,[2] Wayne Phillips,[3] and Martin McMahon[1]

[1]Helen Diller Family Comprehensive Cancer Center, Department of Cell and Molecular Pharmacology, UCSF, San Francisco, California, USA. [2]Department of Dermatology, Yale University School of Medicine, New Haven, Connecticut, USA. [3]Surgical Oncology Research Laboratory, Peter MacCallum Cancer Centre, and Sir Peter MacCallum Department of Oncology, University of Melbourne, Victoria, Australia.

Malignant melanoma is frequently driven by mutational activation of v-raf murine sarcoma viral oncogene homolog B1 (*BRAF*) accompanied by silencing of the phosphatase and tensin homology (*PTEN*) tumor suppressor. Despite the implied importance of PI3K signaling in $PTEN^{Null}$ melanomas, mutational activation of the gene encoding the catalytic subunit of PI3Kα (*PIK3CA*), is rarely detected. Since PTEN has both PI3-lipid phosphatase–dependent and –independent tumor suppressor activities, we investigated the contribution of PI3K signaling to $BRAF^{V600E}$-induced melanomagenesis using mouse models, cultured melanoma cells, and PI3K pathway–targeted inhibitors. These experiments revealed that mutationally activated $PIK3CA^{H1047R}$ cooperates with $BRAF^{V600E}$ for melanomagenesis in mice. Moreover, pharmacological inhibition of PI3Ks prevented growth of $BRAF^{V600E}/PTEN^{Null}$ melanomas in vivo and in tissue culture. Combined inhibition of $BRAF^{V600E}$ and PI3K had more potent effects on the regression of established $BRAF^{V600E}/PTEN^{Null}$ melanomas and cultured melanoma cells than individual blockade of either pathway. Surprisingly, growth of $BRAF^{V600E}/PIK3CA^{H1047R}$ melanomas was dependent on the protein kinase AKT; however, AKT inhibition had no effect on growth of $BRAF^{V600E}/PTEN^{Null}$ melanomas. These data indicate that PTEN silencing contributes a PI3K-dependent, but AKT-independent, function in melanomagenesis. Our findings enhance our knowledge of how $BRAF^{V600E}$ and PI3K signaling cooperate in melanomagenesis and provide preclinical validation for combined pathway–targeted inhibition of PI3K and $BRAF^{V600E}$ in the therapeutic management of $BRAF^{V600E}/PTEN^{Null}$ melanomas.

Introduction

Melanoma is the most deadly form of cutaneous malignancy and is characterized by its increasing incidence, aggressive clinical behavior and propensity for lethal metastasis (1, 2). Although the recent approval of v-raf murine sarcoma viral oncogene homolog B1 (BRAF) pathway–targeted agents such as vemurafenib, dabrafenib, and trametinib is having a marked affect on the treatment of patients with advanced disease, metastatic melanoma remains a challenging malignancy to treat due to intrinsic or acquired resistance to regimens of therapy. Indeed, the onset of acquired drug resistance suggests that combination therapy will be required to achieve durable remission in such patients (3, 4).

Mutational activation of *BRAF* is one of the earliest and most common genetic alterations in human melanoma detected in 50% or more of cases (5). The most common alteration in *BRAF* is a T1799→A transversion in exon 15 resulting in a single amino acid substitution of glutamate (E) for valine (V) at codon 600 (V600E). $BRAF^{V600E}$ is a constitutively active protein kinase, which drives sustained activation of the BRAF/MEK1/2/ERK1/2 MAPK pathway (5).

While mutation of *BRAF* is common in melanoma, expression of $BRAF^{V600E}$ is insufficient for melanomagenesis. Indeed, the vast majority of benign nevi (common moles) express $BRAF^{V600E}$, but these initiated lesions rarely progress to melanoma (6). Expression of $BRAF^{V600E}$ in melanocytes, either in culture or in genetically engineered mouse (GEM) models, indicates that, although melanocytes display an initial burst of proliferation following $BRAF^{V600E}$ expression, they eventually exit the cell division cycle displaying features of a senescence-like growth arrest (7–12). This seemingly powerful barrier to malignant progression must be overcome in order for $BRAF^{V600E}$-expressing melanocytes to progress to malignant melanoma. Consequently, additional alterations are required for the progression of *BRAF*-initiated melanoma.

Silencing of the phosphatase and tensin homology (*PTEN*) tumor suppressor gene on chromosome 10 is a common cooperating event in *BRAF*-mutated melanoma, occurring with a frequency of approximately 30% (13–15). PTEN is a PI3-lipid phosphatase whose principal substrate is the lipid second messenger phosphatidylinositol-3′, 4′,5′-trisphosphate (aka PIP_3). By dephosphorylating PI3-lipids, PTEN suppresses the activity of the PI3K pathway, of which the AKT protein kinases are believed to be key downstream effectors (16).

Given the opposing roles of PTEN and PI3Ks in signaling, it is perhaps surprising that mutational activation of *PIK3CA*, encoding the catalytic subunit of PI3Kα, is rarely detected in melanoma despite its high mutation frequency in other types of human cancer (17–20). This raises the possibility that silencing of PTEN, which has both PI3-lipid phosphatase-dependent and –independent tumor suppressor activities, may not be equivalent to mutational activation of *PIK3CA* (21–25).

Previously, we described a GEM model in which expression of oncogenic $BRAF^{V600E}$ cooperates with PTEN silencing to pro-

Conflict of interest: Martin McMahon receives grant support from Novartis, Plexxicon, GlaxoSmithKline, and Pfizer.

Citation for this article: *J Clin Invest.* 2013;123(12):5104–5118. doi:10.1172/JCI69619.

mote metastatic melanoma (9, 26, 27). Given the low frequency of *PIK3CA* mutations in human melanoma, we resolved to test the role of PI3K signaling in cooperation with mutationally activated $BRAF^{V600E}$ in melanomagenesis. First, using a GEM model, we confirmed that mutationally activated $PIK3CA^{H1047R}$ is sufficient to cooperate with $BRAF^{V600E}$ in melanomagenesis. Moreover, pharmacological inhibition of class 1 PI3Ks (with BKM-120) prevented the growth of $BRAF^{V600E}/PTEN^{Null}$ melanomas. In addition, BKM-120 potentiated the ability of a new $BRAF^{V600E}$ inhibitor (LGX-818) (28, 29) to promote complete regression of established $BRAF^{V600E}/PTEN^{Null}$ melanomas. Finally, we noted a surprising disparity in the sensitivity of $BRAF^{V600E}/PTEN^{Null}$ versus $BRAF^{V600E}/PIK3CA^{H1047R}$ melanomas in their response to pharmacological inhibition of AKT, with the former being insensitive and the latter sensitive to the melanoma-prevention effects of MK-2206. Hence, data presented here support the hypothesis that PI3K activity is essential for the progression and maintenance of $BRAF^{V600E}$-initiated melanoma. Moreover, the data suggest that combined targeting of PI3K may enhance the clinical benefit of pathway-targeted blockade of $BRAF^{V600E}$ signaling in a subset of melanoma patients (3, 30, 31).

Results

Expression of mutationally activated $PIK3CA^{H1047R}$ is sufficient for $BRAF^{V600E}$-initiated melanomagenesis. To test the ability of mutationally activated PIK3CA to drive melanomagenesis, we employed mice carrying a modified *Pik3ca* allele (*$Pik3ca^{lat\text{-}1047R}$*) in which expression of normal PIK3CA is converted to mutationally activated $PIK3CA^{H1047R}$ by Cre recombinase (32). The effects of $PIK3CA^{H1047R}$ expression in melanocytes were compared with PTEN silencing using mice homozygous for a conditional allele of *Pten* (*$Pten^{lox4\text{-}5}$*) (33). In addition, the effects of these mutations were tested in combination with *$BRaf^{CA}$*, a genetically modified *BRaf* allele that allows for Cre-mediated conversion of normal BRAF to $BRAF^{V600E}$ (9, 34). In all cases, melanocyte-specific recombination of loxP-targeted alleles was achieved using a *$Tyr::CreER^{T2}$* transgene (in which Tyr indicates tyrosinase) that is activated by topical application of 4-hydroxytamoxifen (4-HT) to the skin of adult mice (35).

Induced expression of $PIK3CA^{H1047R}$ in the melanocytes of adult *$Tyr::CreER^{T2}$; $Pik3ca^{lat\text{-}1047R}$* mice revealed no discernible phenotype up to 9 months after $PIK3CA^{H1047R}$ expression (not shown). This result is in keeping with a similar lack of phenotype displayed by mice with melanocyte-specific silencing of PTEN (9, 36). In contrast, and as described previously, induced expression of $BRAF^{V600E}$ in the melanocytes of adult *$Tyr::CreER^{T2}$; $BRaf^{CA}$* mice led to development of benign melanocytic nevus–like lesions (Figure 1A and refs. 9–11).

To compare and contrast the ability of $PIK3CA^{H1047R}$ expression or PTEN silencing to cooperate with $BRAF^{V600E}$, adult mice of the appropriate genotype *($Tyr::CreER^{+/0}$;$BRaf^{CA/+}$;$Pik3ca^{lat\text{-}1047R/+}$* or *$Tyr::CreER^{+/0}$;$BRaf^{CA/+}$;$Pten^{lox/lox}$*) were treated topically with 4-HT to initiate melanomagenesis. As expected, $BRAF^{V600E}/PTEN^{Null}$ melanomas became measurable approximately 40 days after initiation and grew inexorably such that 50% of such mice developed end-stage disease (≥1 cm^3), requiring euthanasia by approximately 80 days, and the majority were euthanized by 170 days after initiation (Figure 1, A–C). In contrast, $BRAF^{V600E}/PIK3CA^{H1047R}$ melanomas grew more slowly, becoming measurable around 55 days following initiation (Figure 1, A and B). However, by 200 days, 50% of mice bearing $BRAF^{V600E}/PIK3CA^{H1047R}$ melanomas required euthanasia, and the majority were euthanized by approximately 1 year (Figure 1C).

Visual inspection of $BRAF^{V600E}/PTEN^{Null}$ and $BRAF^{V600E}/PIK3CA^{H1047R}$ melanomas in situ revealed that all tumors displayed areas of variegated pigmentation (Figure 1A), which was confirmed by histological analysis that revealed them to contain both pigmented and amelanotic regions (Figure 1D). The consensus of multiple independent pathologists was that the lesions were representative of melanomas with areas of Schwannian differentiation. Melanoma cells arising in tumors of either genotype stained positive for Ki67, a marker of cell proliferation, as well as S100 and tyrosinase, routinely used markers of melanoma cells (ref. 34 and Supplemental Figure 1; supplemental material available online with this article; doi:10.1172/JCI69619DS1). To profile signal pathway activation in $BRAF^{V600E}/PTEN^{Null}$ or $BRAF^{V600E}/PIK3CA^{H1047R}$ melanomas, immunoblot analysis of proteins extracted from 4 independent tumors of each genotype was performed (Figure 1E). These data indicated that the level of $BRAF^{V600E}$/MEK/ERK or PI3K/AKT pathway activation was equivalent in melanomas of the 2 different genotypes.

To determine whether mice bearing $BRAF^{V600E}/PIK3CA^{H1047R}$ melanomas displayed signs of metastasis, the regional draining lymph nodes were analyzed for the presence of metastatic melanoma cells (Figure 1F). Lymph nodes from mice bearing either $BRAF^{V600E}/PTEN^{Null}$ or $BRAF^{V600E}/PIK3CA^{H1047R}$ melanomas displayed obvious pigmentation, which upon staining with H&E or S100, indicated the presence of islands of metastatic melanoma cells as described previously (9, 27). Hence, $BRAF^{V600E}/PIK3CA^{H1047R}$ melanomas display the ability to metastasize to regional lymph nodes. Consequently, we concluded that $PIK3CA^{H1047R}$ was sufficient to promote the progression of *BRAF*-mutated melanoma in a manner that is similar to that observed with silencing of *PTEN*.

Class 1 PI3K activity is required for $BRAF^{V600E}/PTEN^{Null}$ melanomagenesis. Although mutationally activated $PIK3CA^{H1047R}$ is sufficient to cooperate with $BRAF^{V600E}$ for melanoma progression, these data do not formally demonstrate that PI3K activity is required for the growth of $BRAF^{V600E}/PTEN^{Null}$ melanomas. To assess this, we tested the ability of a pharmacological inhibitor specific for class I PI3Ks, BKM-120 (37), which lacks activity against the mTORC1/2 complex, to prevent the growth of *BRAF* mutated melanomas. To do so, $BRAF^{V600E}/PTEN^{Null}$ or $BRAF^{V600E}/PIK3CA^{H1047R}$ melanomas were initiated on the back skin of adult mice of the appropriate genotype by topical application of 4-HT. Approximately 4 weeks later, a time when initiated melanomas are visible but not yet measurable, we commenced oral administration of BKM-120. Compared with vehicle control, mice treated with BKM-120 displayed attenuated growth of both $BRAF^{V600E}/PTEN^{Null}$ and $BRAF^{V600E}/PIK3CA^{H1047R}$ melanomas (Figure 2, A and B). The potent antimelanoma activity of BKM-120 was particularly striking against $BRAF^{V600E}/PTEN^{Null}$ melanomas after 58 or 65 days of treatment (Figure 2, A and C; $^*P < 0.01$). The preventative effects of BKM-120 on $BRAF^{V600E}/PIK3CA^{H1047R}$ melanomas did not reach statistical significance because the treatment schedule was ended before the vehicle-treated mice had all developed end-stage disease. However, a strong trend toward smaller tumors was detected, as would be expected of melanomas promoted by mutational activation of *Pik3ca* (Figure 2, B and D). At euthanasia, tumors were stained with either H&E or antisera against S-100, and they displayed similar char-

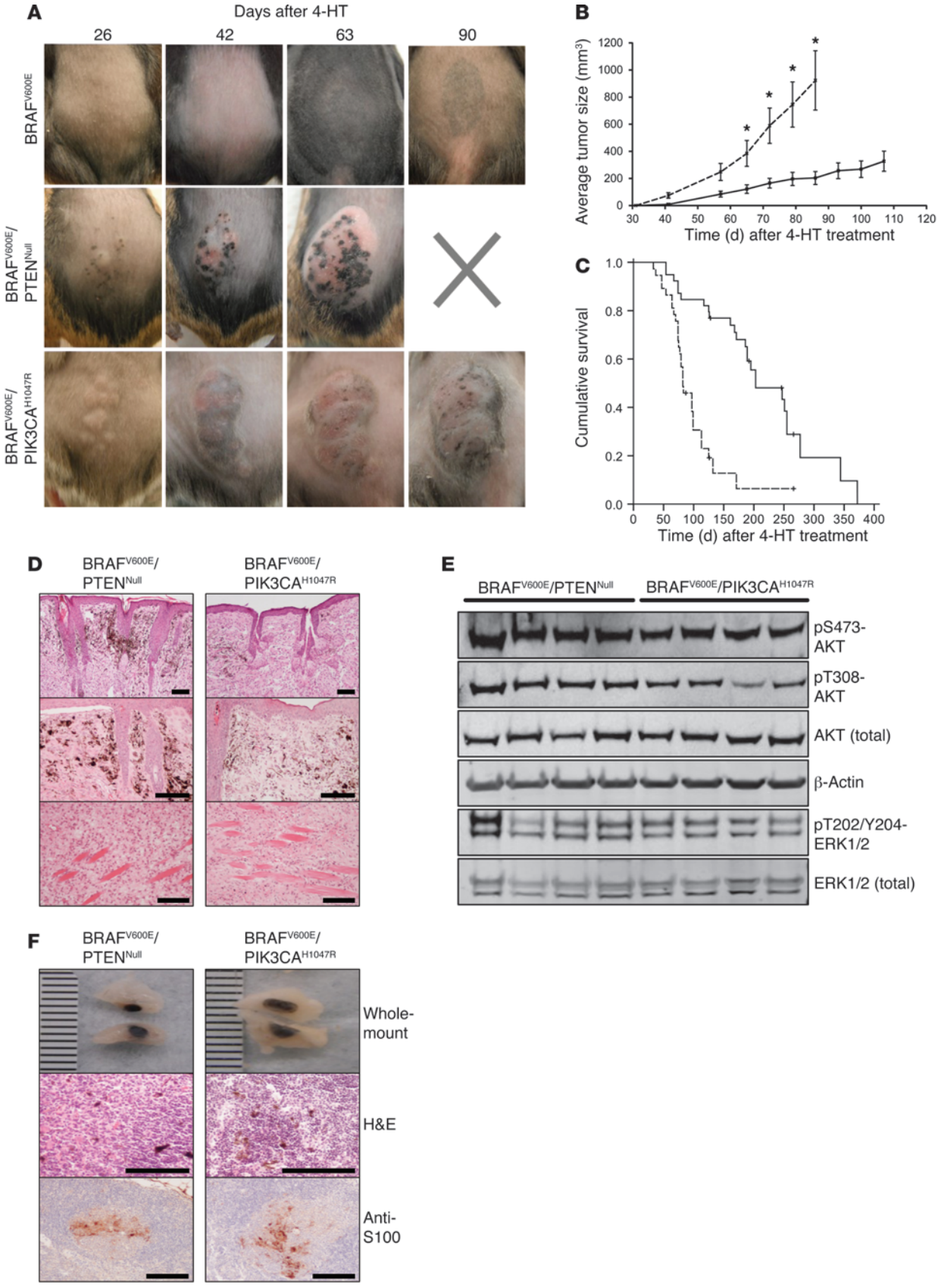
A
Days after 4-HT
26
42
63
90
BRAF V600E
BRAF V600E/ PTEN Null
BRAF V600E/ PIK3CA H1047R
B
Average tumor size (mm3)
Time (d) after 4-HT treatment
C
Cumulative survival
Time (d) after 4-HT treatment
D
BRAF V600E/ PTEN Null
BRAF V600E/ PIK3CA H1047R
E
BRAF V600E/PTEN Null
BRAF V600E/PIK3CA H1047R
pS473-AKT
pT308-AKT
AKT (total)
β-Actin
pT202/Y204-ERK1/2
ERK1/2 (total)
F
BRAF V600E/ PTEN Null
BRAF V600E/ PIK3CA H1047R
Whole-mount
H&E
Anti-S100

Figure 1
Expression of PIK3CA^{H1047R} cooperates with BRAF^{V600E} in melanomagenesis. (**A**) Recombination was initiated in *Tyr::CreER* mice carrying *BRaf^{CA}* (BRAF^{V600E}) or a combination of *BRaf^{CA}* with either *Pten$^{lox4\text{-}5/lox4\text{-}5}$* (BRAF^{V600E}/PTEN^{Null}) or *Pik3ca$^{lat\text{-}1047R/+}$* (BRAF^{V600E}/PIK3CA^{H1047R}) by topical 4-HT application, and melanoma initiation was assessed for up to 90 days. (**B**) Growth rate of BRAF^{V600E}/PTEN^{Null} (n = 10) (dashed line) versus BRAF^{V600E}/PIK3CA^{H1047R} (n = 10) (solid line) melanomas. Average tumor sizes (mm^3 ± SEM) were measured starting at 30 days following 4-HT induction. *P < 0.01, Student's 1-tailed t test. (**C**) Kaplan-Meier survival analysis of mice bearing BRAF^{V600E}/PTEN^{Null} (n = 37, dashed line) or BRAF^{V600E}/PIK3CA^{H1047R} melanomas (n = 39, solid line). Median survival times were 203 and 82 days after 4HT administration respectively (Mantel-Cox log-rank test, P < 0.01). (**D**) H&E staining revealed melanomas arising in BRAF^{V600E}/PTEN^{Null} or BRAF^{V600E}/PIK3CA^{H1047R} mice to be histopathologically heterogeneous (top panels). Tumors of both genotypes comprised pigmented and nonpigmented cells (middle panels), and invasion through the musculature was frequently identified (bottom panels). (**E**) Tumor lysates of BRAF^{V600E}/PTEN^{Null} or BRAF^{V600E}/PIK3CA^{H1047R} melanomas were probed with backbone- or phospho-specific antisera against the various indicated proteins. β-actin was used as a loading control. (**F**) Regional draining lymph nodes of mice bearing BRAF^{V600E}/PTEN^{Null} or BRAF^{V600E}/PIK3CA^{H1047R} melanomas were found to be pigmented. H&E staining (middle panel) revealed the majority of pigmentation present was associated with melanophages; however, the structure of the lymph node was disrupted, suggesting the presence of tumor cells. Anti-S100 immunostaining (bottom panel) revealed clusters of positive cells. Scale bars: 100 μm. Scale bars rule (on whole-mount images) shows measurement in mm.

acteristics regardless of whether they were vehicle or BKM-120 treated (Figure 2E). Moreover, staining revealed the presence of Ki67-positive cells, indicating that this regime of PI3K inhibitor treatment did not completely abolish the proliferation of these lesions. As a pharmacodynamic marker of the response of either BRAF^{V600E}/PTEN^{Null} or BRAF^{V600E}/PIK3CA^{H1047R} melanomas to BKM-120, whole-tumor lysates were analyzed by immunoblot with antisera against pS473-AKT (Figure 2F). As expected, AKT phosphorylation was decreased in BKM-120–treated mice regardless of genotype, whereas no effect on phospho-ERK1/2 (pT202/Y204) was detected. These data therefore indicate that class I PI3K activity is required for BRAF^{V600E}/PTEN^{Null} melanomagenesis and, in concert with the results described above, indicate that PI3K activity is both necessary and sufficient to promote the growth of *BRAF* mutated melanoma.

BRAF^{V600E}/PTEN^{Null} melanomas grow despite AKT inhibition. Although the AKT1-3 protein kinases are believed to be important effectors of PI3-lipid signaling, there are numerous PI3-lipid–binding proteins in cells including the SGK and TEC family of protein kinases as well as multiple regulators of guanine nucleotide exchange/hydrolysis of RAS family GTPases (38). Hence, to test the importance of AKT activity in melanomagenesis, we utilized MK-2206 (MK), an allosteric inhibitor of AKT1-3 activation, in conjunction with the mouse models described above (39). As described above, BRAF^{V600E}/PTEN^{Null} or BRAF^{V600E}/PIK3CA^{H1047R} melanomas were initiated in adult mice, which were then administered MK-2206 in the prevention setting to test the importance of AKT1-3 for melanoma progression.

Upon treatment of incipient BRAF^{V600E}/PTEN^{Null} melanomas with MK-2206, no clear impact on macroscopic tumor growth was observed compared with vehicle-treated controls (Figure 3A). Measurement and quantification of tumor volumes revealed that, while MK-2206–treated BRAF^{V600E}/PTEN^{Null} melanomas displayed a trend toward smaller size compared with vehicle controls, there was no statistically significant difference in tumor size even after almost 8 weeks of drug administration (Figure 3C). Indeed, many of the MK-2206–treated BRAF^{V600E}/PTEN^{Null} melanoma–bearing mice developed end-stage disease requiring euthanasia while receiving drug treatment. In contrast, treatment of BRAF^{V600E}/PIK3CA^{H1047R} melanoma-bearing mice with an identical dosing regimen of MK-2206 was highly effective in preventing the growth of incipient tumors (Figures 3, B and D). In this case, measurement of tumor volumes revealed that the difference between MK-2206 and vehicle-treated controls was statistically significant at 76, 83, and 90 days following the onset of drug administration (P < 0.01) (Figure 3D).

Histopathological analysis of MK-2206–treated melanomas indicated that they displayed staining characteristics (H&E, S-100, Ki67) similar to those of their vehicle-treated counterparts (Figure 3E) and similar to those of entirely untreated mice (Figure 1D and Supplemental Figure 1). Immunoblot analysis of whole-tumor lysates revealed that AKT phosphorylation was indeed inhibited in both BRAF^{V600E}/PTEN^{Null} and BRAF^{V600E}/PIK3CA^{H1047R} melanomas exposed to MK-2206, indicating that the drug had its predicted on-target effects in melanomas of either genotype (Figure 3F). Furthermore, we also found established BRAF^{V600E}/PIK3CA^{H1047R} melanomas to show a cytostatic response to MK-2206 treatment in the therapy setting (Supplemental Figure 2). These data therefore indicate that BRAF^{V600E}/PIK3CA^{H1047R} melanoma growth is AKT dependent, but suggest that the growth of BRAF^{V600E}/PTEN^{Null} melanomas is significantly less dependent on signaling mediated by AKT.

Proliferation of mouse and human BRAF-mutated melanoma cell lines is attenuated by PI3K inhibition. To extend observations made with GEM models in vivo, we tested the efficacy of pathway-targeted inhibitors using cultured mouse or human BRAF^{V600E}-expressing melanoma cells lines. For these experiments, we established several new cell lines from our GEM models. We noted that efficient establishment of BRAF^{V600E}-expressing mouse melanoma cell lines requires silencing of the p16^{INK4A} and p19^{ARF} tumor suppressors encoded at the *Cdkn2a* locus. Consequently, we employed a Cre-inactivated allele of *Cdkn2a* in conjunction with the genetic manipulations described above to first generate BRAF^{V600E}/PTEN^{Null}/CDKN2A^{Null} or BRAF^{V600E}/PIK3CA^{H1047R}/CDKN2A^{Null} melanomas from which cell lines were derived as described in the Methods (40). Analysis of these mouse melanoma–derived cell lines indicated that they contained the engineered genetic alterations. We also tested the response of the human BRAF^{V600E}/PTEN^{Null} melanoma cell line 1205Lu (41). These cells are a derivative of WM793 cells, but have enhanced tumorigenic potential when implanted into immunocompromised mice (42).

To test effects of BRAF^{V600E}/MEK/ERK blockade on proliferation, mouse melanoma cell lines were treated with pathway-targeted inhibitors for 3 days with cell number quantified every 24 hours (Figure 4A). As expected, pharmacological blockade of BRAF^{V600E} (GSK2118436), MEK1/2, (PD0325901) or ERK1/2 (SCH772984) elicited antiproliferative effects on melanoma cells regardless of their PTEN or PIK3CA status (43–45). Similar to mouse BRAF^{V600E}-expressing melanoma cells, treatment of 1205Lu cells with BRAF^{V600E}, MEK1/2, or ERK1/2 inhibitors for 6 days indicated that these agents had a predominantly cytostatic effect on cell proliferation compared with DMSO-treated controls (Figure 4A). To test the importance of PI3K/AKT signaling, we employed 2 structurally dis-

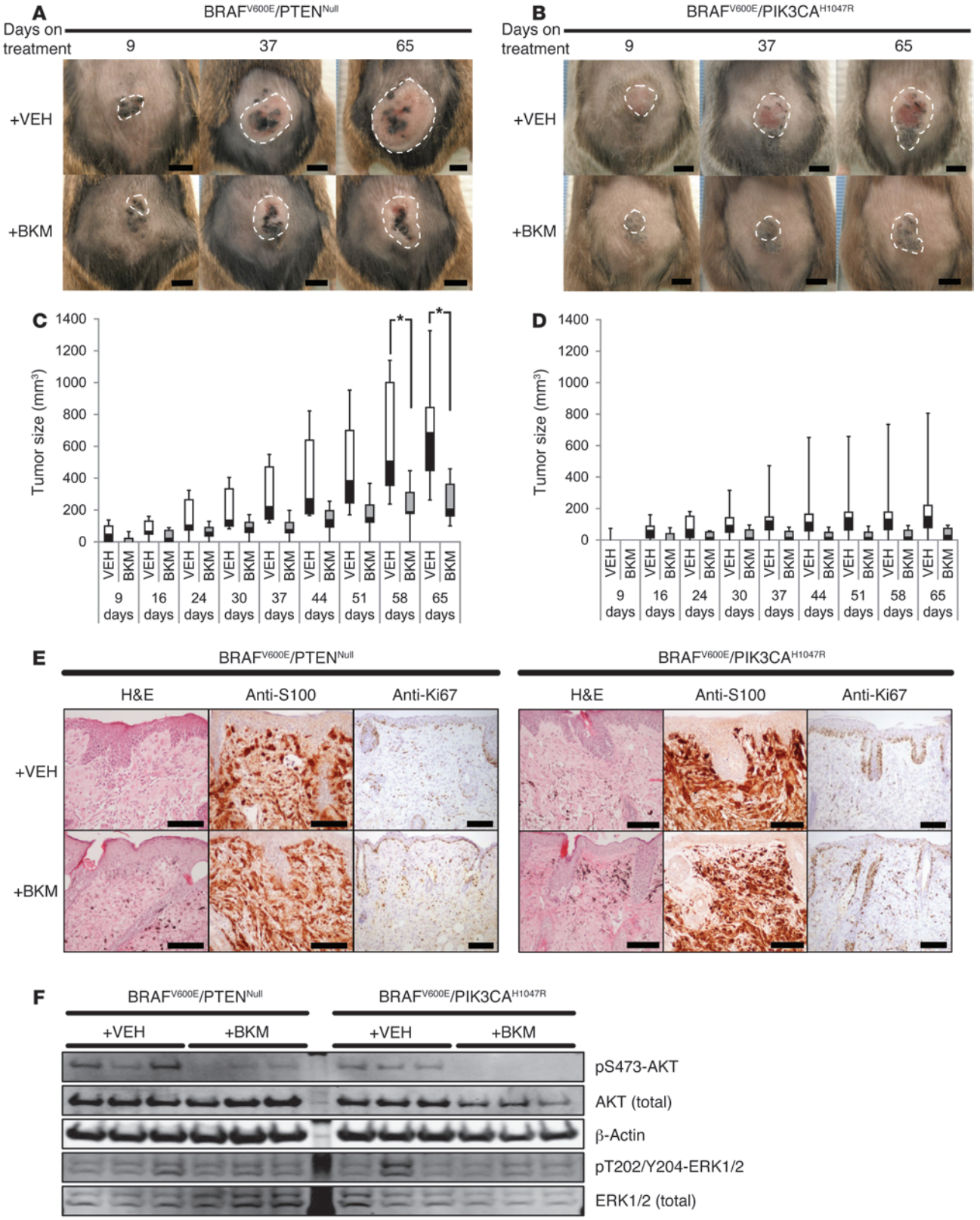
A
BRAF^V600E/PTEN^Null
Days on treatment
9
37
65
+VEH
+BKM
B
BRAF^V600E/PIK3CA^H1047R
Days on treatment
9
37
65
+VEH
+BKM
C
Tumor size (mm³)
1400
1200
1000
800
600
400
200
0
*
*
VEH
BKM
9 days
16 days
24 days
30 days
37 days
44 days
51 days
58 days
65 days
D
Tumor size (mm³)
1400
1200
1000
800
600
400
200
0
VEH
BKM
9 days
16 days
24 days
30 days
37 days
44 days
51 days
58 days
65 days
E
BRAF^V600E/PTEN^Null
BRAF^V600E/PIK3CA^H1047R
H&E
Anti-S100
Anti-Ki67
+VEH
+BKM
F
BRAF^V600E/PTEN^Null
BRAF^V600E/PIK3CA^H1047R
+VEH
+BKM
+VEH
+BKM
pS473-AKT
AKT (total)
β-Actin
pT202/Y204-ERK1/2
ERK1/2 (total)

Figure 2
$BRAF^{V600E}/PTEN^{Null}$ melanoma development is PI3K dependent. $BRAF^{V600E}/PTEN^{Null}$ (**A**) or $BRAF^{V600E}/PIK3CA^{H1047R}$ (**B**) melanoma growth was initiated, and 30 days later, treatment with vehicle control (+VEH) or with the PI3K inhibitor BKM-120 (+BKM) was initiated ($BRAF^{V600E}/PTEN^{Null}$ + VEH, $n = 8$; $BRAF^{V600E}/PTEN^{Null}$ + BKM, $n = 7$; $BRAF^{V600E}/PIK3CA^{H1047R}$ + VEH, $n = 6$; $BRAF^{V600E}/PIK3CA^{H1047R}$ + BKM, $n = 6$). Melanoma growth was visually assessed over the course of treatment. White dashed lines indicate tumor borders; note that areas of pigmentation are not necessarily indicative of tumor size and tumor depth is not readily apparent from the photographs. Scale bars: 5 mm. (**C** and **D**) Melanoma growth in the absence (VEH) or presence of PI3K inhibitor (BKM) was measured from 9–65 days after commencement of treatment. BKM-120–treated $BRAF^{V600E}/PTEN^{Null}$ melanomas were significantly smaller than vehicle-treated controls from 58 days on treatment onwards (*$P < 0.01$, Student's 1-tailed t test) (**C**). BKM-120 treatment suppressed $BRAF^{V600E}/PIK3CA^{H1047R}$ melanoma growth, although this was not statistically significant due to large variation in the vehicle-treated control group (**D**). (**E**) $BRAF^{V600E}/PTEN^{Null}$ or $BRAF^{V600E}/PIK3CA^{H1047R}$ melanomas from either vehicle- or BKM-120–treated mice were stained with H&E, anti-S100, or anti-Ki67 as indicated. Scale bars: 100 μm. (**F**) Tumor lysates obtained from vehicle- or BKM-120–treated $BRAF^{V600E}/PTEN^{Null}$ or $BRAF^{V600E}/PIK3CA^{H1047R}$ melanomas were probed with backbone- or phospho-specific antisera against the various indicated proteins. β-Actin was used as a loading control.

tinct inhibitors of either class 1 PI3Ks (GDC-0941 and BKM-120) (46, 47) or AKT1-3 (MK-2206 and GSK690693) (39, 48, 49). Indeed, the AKT inhibitors are also mechanistically dissimilar in that MK-2206 is an allosteric inhibitor that prevents membrane recruitment and therefore AKT phosphorylation. In contrast, GSK690693 is a conventional ATP competitive inhibitor that leads to accumulation of inactive but highly phosphorylated AKT.

In general, $BRAF^{V600E}/PIK3CA^{H1047R}$ mouse melanoma cells were more sensitive to PI3K/AKT blockade compared with their $BRAF^{V600E}/PTEN^{Null}$ counterparts such that the proliferation of $BRAF^{V600E}/PIK3CA^{H1047R}$ melanoma cells was potently suppressed by treatment with both PI3K inhibitors and by one of the AKT inhibitors. Perhaps surprisingly, the second AKT inhibitor had a less profound effect upon the proliferation of $BRAF^{V600E}/PIK3CA^{H1047R}$ melanoma cells compared with the other agents, but still significantly reduced proliferation compared with DMSO-treated controls (Figure 4A). In contrast, and consistent with in vivo observations, $BRAF^{V600E}/PTEN^{Null}$ cells were relatively insensitive to inhibition with either of the AKT inhibitors and were also less sensitive to one of the PI3K inhibitors (GDC-0941). However, $BRAF^{V600E}/PTEN^{Null}$ cells were highly sensitive to BKM-120, which resulted in decreased cell number over the course of the experiment.

GDC-0941-mediated inhibition of PI3K activity in 1205Lu cells elicited a cytostatic effect on cell growth, whereas treatment with BKM-120 resulted in a clear decrease in cell number over the course of the experiment. However, the cytotoxic effects of BKM-120 at higher concentrations compared with GDC-0941 may reflect a known off-target effect of the agent on microtubule polymerization and so must be viewed with caution (50). Treatment of 1205Lu cells with either of the AKT inhibitors also resulted in reduced cell proliferation, though treatment with either AKT inhibitor was less effective at suppressing cell growth compared with $BRAF^{V600E}$, MEK, or ERK inhibitors. The longer term effects of these agents was assessed by treating all of the melanoma cell lines with the listed agents for 6 days, at which time the cells were fixed and stained with crystal violet. Under these conditions, the dramatic inhibitory effect of BKM-120 on melanoma cell growth was readily apparent across all 3 cell lines tested (Figure 4B).

Immunoblot analysis of extracts of control (DMSO treated) versus drug-treated $BRAF^{V600E}/PTEN^{Null}$ or $BRAF^{V600E}/PIK3CA^{H1047R}$ mouse melanoma cells as well as 1205Lu human melanoma cells was performed to confirm on-target effects of the various agents employed (Figure 4C). As expected, treatment with $BRAF^{V600E}$ (GSK36), MEK (PD), or ERK (SCH) inhibitors inhibited phosphorylation of ERK1/2 (pT202/Y204), which was accompanied by elevated expression of BIM, a proapoptotic BCL-2 family member and known target of ERK1/2 signaling in melanoma cells (51). Inhibition of $BRAF^{V600E}$/MEK/ERK signaling had no obvious effect on pS473-AKT. In contrast, treatment of melanoma cells with either PI3K or AKT inhibitors led to reduced levels of phosphorylated pS473-AKT, with the exception of GSK690693 (GSK93), which elicited elevated pAKT due to its mechanism of action (49). The durability of the inhibitory effects of the various AKT or class 1 PI3K inhibitors on pS473-AKT was tested after a single administration of drug to mouse $BRAF^{V600E}/PTEN^{Null}$ or $BRAF^{V600E}/PIK3CA^{H1047R}$ mouse melanoma cells for 24–72 hours (Supplemental Figure 3). As expected, a single administration of any one of these agents elicited durable inhibition of pS473-AKT over the course of 72 hours.

PI3K inhibition enhances $BRAF^{V600E}$ inhibition to suppress growth of BRAF-mutated melanoma cells in vitro. Since mutationally activated BRAF cooperates with PI3K pathway activation to promote melanomagenesis in vivo, we wished to determine whether pharmacological inhibition of class I PI3Ks (BKM-120) might enhance the antimelanoma effects of a new $BRAF^{V600E}$ selective inhibitor (LGX-818) in vitro (28, 29). To do so, human or mouse melanoma cell lines described above were treated with a range of concentrations of BKM-120 (from 0–5 μM) or with LGX-818 (from 0–10 μM) either alone or in combination to assess possible synergistic effects of these agents against melanoma cells based on the methods of Chou and Talalay (ref. 52 and Supplemental Figure 4, A and B). To simplify further experiments, we used the results of this analysis to choose a single dose combination (320 nM BKM-120 and 80 nM LGX-818), which was predicted to be synergistic. Cells were grown in the presence of drugs, either as single agents or in combination, for 3 days with viable cells enumerated every 24 hours (Figure 5A). This revealed that, in all cell lines, there was a trend toward combination treatment being more effective at inhibiting cell growth compared with single-agent treatment, although this was not statistically significant in any case.

To examine the biochemical effects of single-agent versus combination BKM-120 or LGX-818 treatment, lysates from human or mouse melanoma cells treated for 24 hours with either DMSO control, BKM-120 alone (low dose of 320 nM or high dose of 5 μM), LGX-818 alone (low dose of 80 nM or high dose of 1 μM) or both agents (combination of low doses or high doses) were analyzed by immunoblotting (Figure 5B). As expected, treatment of cells with BKM-120 inhibited pS473-AKT and pPRAS40,with the strongest inhibitory effect observed with the higher dose of drug. Perhaps surprisingly, BKM-120 treatment elicited a modest but reproducible increase in levels of pERK1/2. LGX-818 inhibited pERK1/2, leading to elevated expression of BIM with equal efficiency at both doses. In contrast to the effects of BKM-120 on pERK1/2, LGX-818 had no effect on pS473-AKT. Analysis of downstream

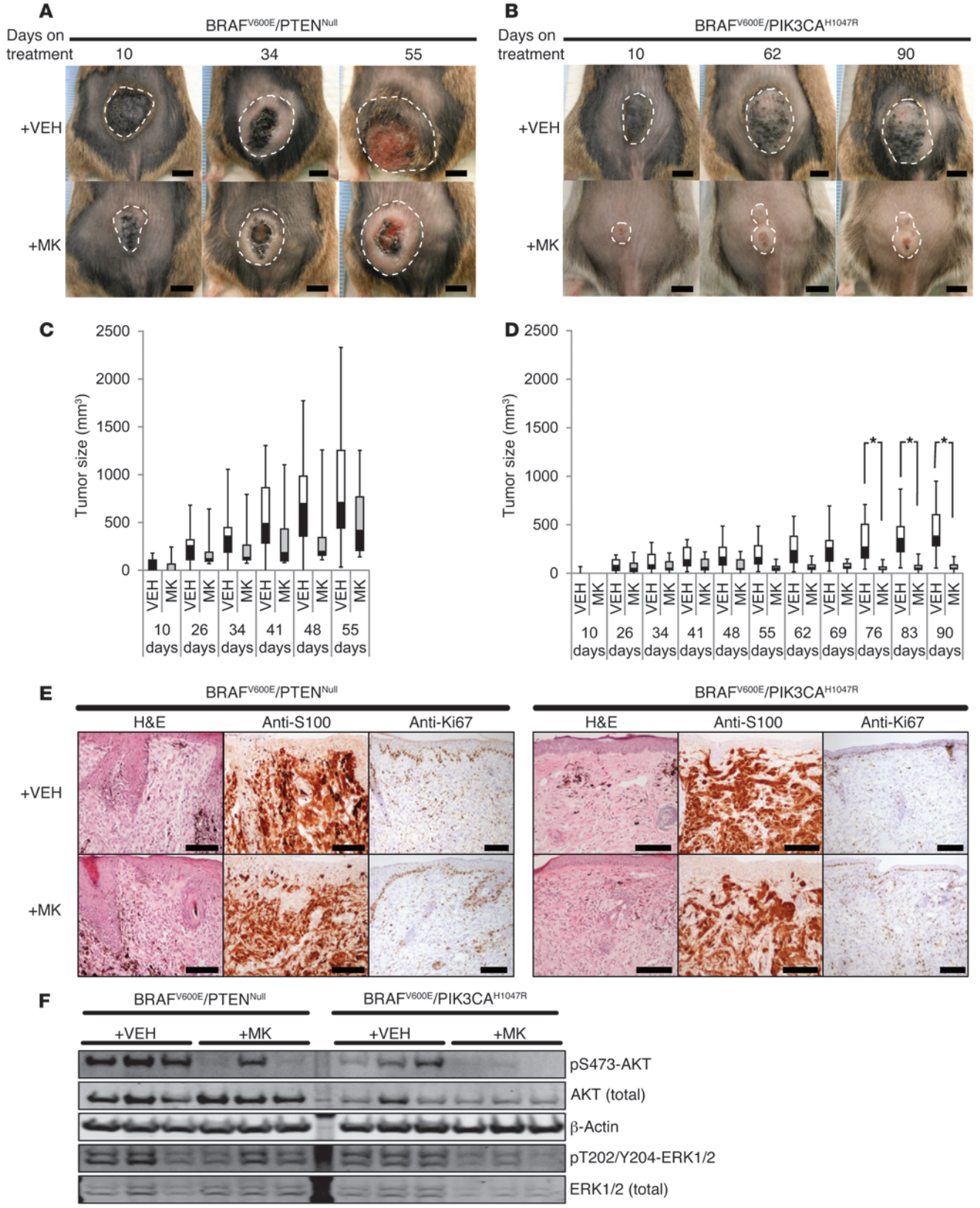
A
BRAF^V600E/PTEN^Null
Days on treatment
10
34
55
+VEH
+MK
B
BRAF^V600E/PIK3CA^H1047R
Days on treatment
10
62
90
+VEH
+MK
C
Tumor size (mm³)
2500
2000
1500
1000
500
0
VEH
MK
10 days
26 days
34 days
41 days
48 days
55 days
D
Tumor size (mm³)
10 days
26 days
34 days
41 days
48 days
55 days
62 days
69 days
76 days
83 days
90 days
*
E
BRAF^V600E/PTEN^Null
BRAF^V600E/PIK3CA^H1047R
H&E
Anti-S100
Anti-Ki67
+VEH
+MK
F
BRAF^V600E/PTEN^Null
BRAF^V600E/PIK3CA^H1047R
+VEH
+MK
+VEH
+MK
pS473-AKT
AKT (total)
β-Actin
pT202/Y204-ERK1/2
ERK1/2 (total)

Figure 3
AKT activity is required for $BRAF^{V600E}/PIK3CA^{H1047R}$ but not $BRAF^{V600E}/PTEN^{Null}$ melanoma growth. $BRAF^{V600E}/PTEN^{Null}$ (**A**) or $BRAF^{V600E}/PIK3CA^{H1047R}$ (**B**) melanoma growth was initiated, and 30 days later, treatment with vehicle control (+VEH) or with MK-2206, a pan-AKT inhibitor (+MK) was begun ($BRAF^{V600E}/PTEN^{Null}$ + VEH, n = 10; $BRAF^{V600E}/PTEN^{Null}$ + MK, n = 8; $BRAF^{V600E}/PIK3CA^{H1047R}$ + VEH, n = 10, $BRAF^{V600E}/PIK3CA^{H1047R}$ + MK, n = 10). Melanoma growth was visually assessed over the treatment time as described above. (**C** and **D**) Melanoma growth in the absence (VEH) or presence of AKT inhibitor (MK) was measured from 10–90 days after commencement of treatment. MK-2206–treated $BRAF^{V600E}/PTEN^{Null}$ melanomas were not significantly smaller than vehicle-treated controls at any time after initiation of drug treatment (Student's 1-tailed t test, **C**). In contrast, $BRAF^{V600E}/PIK3CA^{H1047R}$ melanomas were significantly smaller in MK-2206–treated mice compared with vehicle treated from day 76 of treatment onwards (*$P < 0.01$, Student's 1-tailed t test, *$P < 0.01$, **D**). (**E**) $BRAF^{V600E}/PTEN^{Null}$ or $BRAF^{V600E}/PIK3CA^{H1047R}$ melanomas from either vehicle- or MK-2206–treated mice were stained with H&E, anti-S100, or anti-Ki67 as indicated. Scale bars: 100 μm. (**F**) Tumor lysates obtained from vehicle- or MK-2206–treated $BRAF^{V600E}/PTEN^{Null}$ or $BRAF^{V600E}/PIK3CA^{H1047R}$ melanomas were probed with backbone- or phospho-specific antisera against AKT or ERK1/2. β-Actin was used as a loading control.

signaling events revealed a greater decrease in the phosphorylation of ribosomal protein S6 (pRP-S6) and eIF4E binding protein 1 (4E-BP1) in cells treated with combination BKM-120 plus LGX-818 compared with effects observed with the same drug doses as single agents. Furthermore, induction of apoptosis, as inferred by the presence of cleaved caspase 3 (CC3), was most readily detected in cells that received high-dose LGX-818 plus BKM-120 in combination compared with the relevant single-agent treatments or DMSO controls. These data therefore suggest that inhibition of both PI3K and $BRAF^{V600E}$ in mouse or human melanoma cells in vitro has a cooperative inhibitory effect on downstream signaling pathways and on the induction of machinery of apoptosis.

PI3K inhibition has modest antimelanoma therapeutic activity in vivo, but promotes regression of established tumors in response to $BRAF^{V600E}$ inhibition with LGX-818. Given the potent antimelanoma preventive effects in vivo and antiproliferative effects in vitro of BKM-120–mediated PI3K inhibition, we wished to test the efficacy of this agent in promoting the regression of established melanomas in our GEM models. $BRAF^{V600E}/PTEN^{Null}$ or $BRAF^{V600E}/PIK3CA^{H1047R}$ melanomas were initiated on the back skin of adult mice of the appropriate genotype as described before. As melanomas developed, their volumes were estimated weekly until the mean tumor size of the group exceeded 500 mm^3. At this point, mice were assigned to treatment groups such that tumors were equally distributed between groups based on their size and on mouse sex. Mice were then orally administered with either vehicle or BKM-120 (30 mg/kg/d) as described for the melanoma prevention studies. Mice were dosed continuously until their tumor size exceeded 1000 mm^3, with the experiment terminated for analysis when fewer than 3 mice remained in either the vehicle- or drug-treated groups.

Upon administration of BKM-120, very modest growth suppression of $BRAF^{V600E}/PIK3CA^{H1047R}$ or $BRAF^{V600E}/PTEN^{Null}$ (Supplemental Figure 5, A and B) melanomas was visually noted. Measurement of tumor sizes (Figure 6, A and C) revealed that, while there was indeed a trend toward reduced tumor growth upon BKM-120 treatment in both $BRAF^{V600E}/PTEN^{Null}$ (Figure 6C) and $BRAF^{V600E}/PIK3CA^{H1047R}$ (Figure 6A) melanomas, this difference was not statistically significant at any time point within the study.

To assess the effects of therapeutic BKM-120 treatment upon PI3K pathway activity in melanomas, we performed immunoblotting analysis of tumor lysates. Mice bearing $BRAF^{V600E}/PTEN^{Null}$ or $BRAF^{V600E}/PIK3CA^{H1047R}$ melanomas were euthanized 4 hours after a final dose of BKM-120 or vehicle treatment. At this time point, activation of the PI3K/AKT pathway, as assessed by detection of phosphorylated AKT (pS473-AKT), was found to be strongly suppressed in mice treated with BKM-120 compared with vehicle control (Figure 6B). This effect was readily observed in both $BRAF^{V600E}/PTEN^{Null}$- and $BRAF^{V600E}/PIK3CA^{H1047R}$-expressing melanomas. Additionally, to assess the pharmacodynamic profile of PI3K pathway inhibition with BKM-120, we treated several mice bearing $BRAF^{V600E}/PIK3CA^{H1047R}$ melanomas and euthanized them either 8 or 16 hours after drug administration. This analysis indicated that, although an appreciable reduction in levels of activated AKT was detected 8 hours after BKM-120 treatment, by 16 hours, the level of pS473-AKT was restored to that of vehicle-treated controls (Figure 6B). These data are consistent with previous pharmacodynamic analysis of BKM-120 bioavailability in mice bearing xenografted tumors (53). Thus, using this dosing regimen, we noted only transient inhibition of PI3K/AKT signaling, which may be insufficient to elicit regression of $BRAF^{V600E}/PTEN^{Null}$ or $BRAF^{V600E}/PIK3CA^{H1047R}$ melanomas. We additionally analyzed the effects of BKM-120 treatment upon growth of xenografted human 1205Lu melanoma cells implanted into immunocompromised mice. We found the results of these experiments to mirror those in the autochthonous GEM models, with BKM-120 treatment having no therapeutic effect on established tumors despite the detection of reduced intratumoral pAKT-S473 levels (Supplemental Figure 5, C and D).

Given the in vitro evidence for synergy between PI3K and $BRAF^{V600E}$ inhibition with BKM-120 and LGX-818 respectively, we tested the antimelanoma activity of these agents in the therapy setting against established autochthonous $BRAF^{V600E}/PTEN^{Null}$ melanomas in vivo. $BRAF^{V600E}/PTEN^{Null}$ melanomas were induced on the back skin of 24 adult mice as described above and measured weekly until the mean tumor size of the group exceeded 500 mm^3. Mice were then assigned to treatment groups of 6 mice per group such that tumors were equally distributed between groups based on their size and on mouse sex. Mice were then administered the following: (a) vehicle control; (b) LGX-818 (30 mg/kg/d); (c) BKM-120 (30 mg/kg/d); or (d) LGX-818 plus BKM-120 (30 mg/kg/d dosed together) for a continuous dosing period of 50 days, with tumor size measured on a weekly basis.

In contrast to the lack of tumor regression observed with BKM-120 described above, single-agent LGX-818 elicited striking tumor regression that was readily detected within 7 days following drug administration and that continued for the full 50 days of drug administration (Figure 6C). However, when BKM-120 was coadministered with LGX-818, we noted that melanomas regressed more quickly than with single agent LGX-818. The difference between single-agent LGX-818 and combination therapy was statistically significant at days 9–18 and day 29 of treatment ($P < 0.01$).

To further examine the effect of the various interventions on tumor growth/regression, we generated a waterfall plot of the response of individual mice to BKM-120 or LGX-818 as single agents or in combination (Figure 6D). Animals that displayed progressive disease in which tumor size doubled over the course

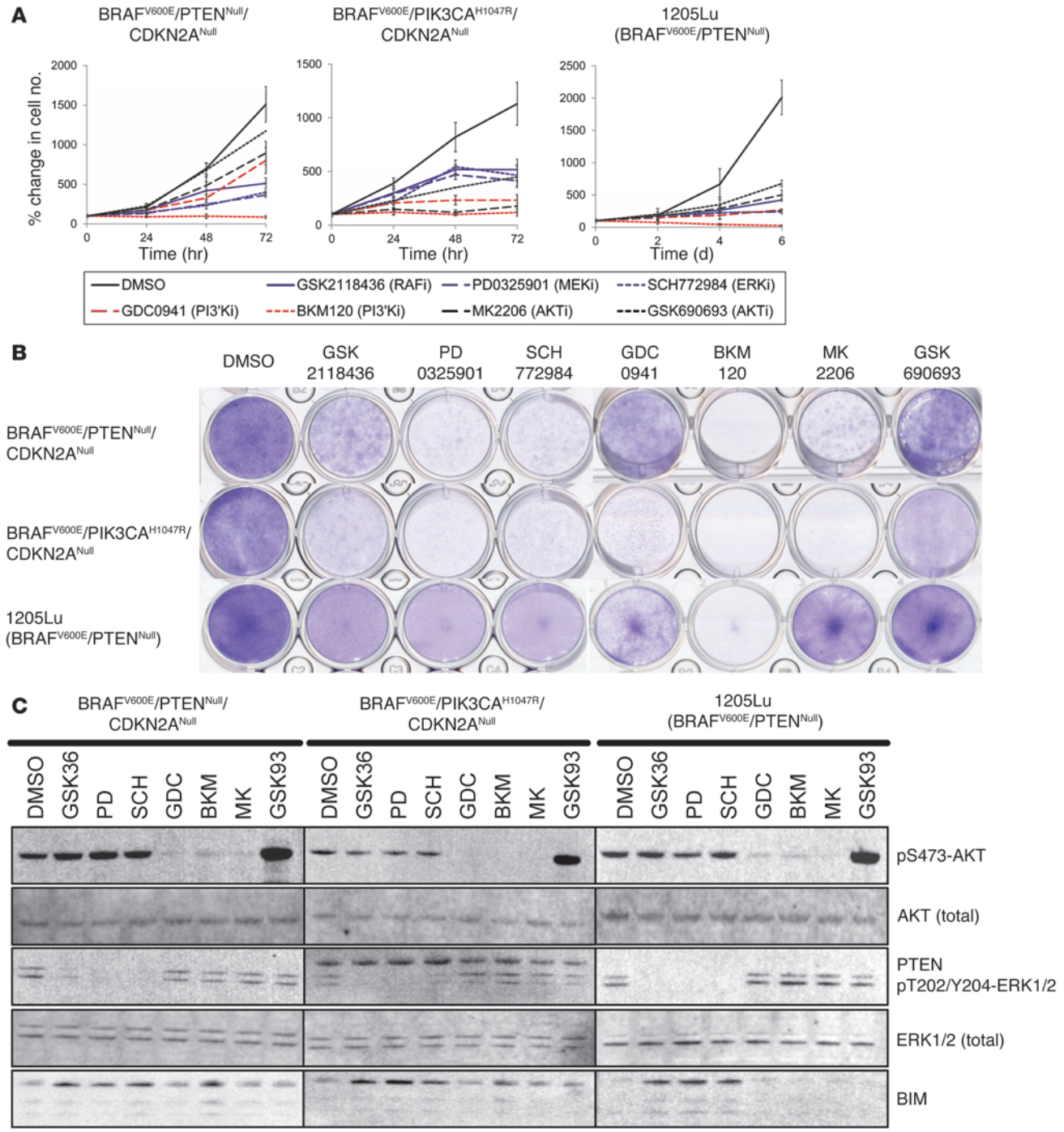

Figure 4

Melanoma-derived cell lines of mouse or human origin are sensitive to PI3K inhibition by BKM-120 in vitro. (**A**) Cells derived from mouse BRAF^{V600E}/PTEN^{Null}/CDKN2A^{Null} melanomas (left), BRAF^{V600E}/PIK3CA^{H1047R}/CDKN2A^{Null} melanomas (center), or the human melanoma cell line 1205Lu (BRAF^{V600E}, PTEN^{Null}) (right) were treated with pathway-targeted inhibitors as indicated, and cells counted either every 24 hours for a total period of 72 hours (mouse BRAF^{V600E}/PTEN^{Null}/CDKN2A^{Null} and BRAF^{V600E}/PIK3CA^{H1047R}/CDKN2A^{Null} cells) or every 2 days for a total period of 6 days (human 1205Lu cells). Cell counts are indicated as percentage change in cell number, with error bars plotted showing SD of the data. (**B**) Mouse and human melanoma cell lines were grown in the presence of the indicated inhibitors for a period of 6 days before being stained with crystal violet to visualize cell growth. (**C**) Cell lysates were obtained from mouse BRAF^{V600E}/PTEN^{Null}/CDKN2A^{Null} or BRAF^{V600E}/PIK3CA^{H1047R}/CDKN2A^{Null} melanoma cell lines or human 1205Lu melanoma cells treated with the indicated targeted therapeutics for 24 hours. Lysates were probed with the antisera indicated to assess effective inhibition of targets and downstream responses in the presence of drug compounds.

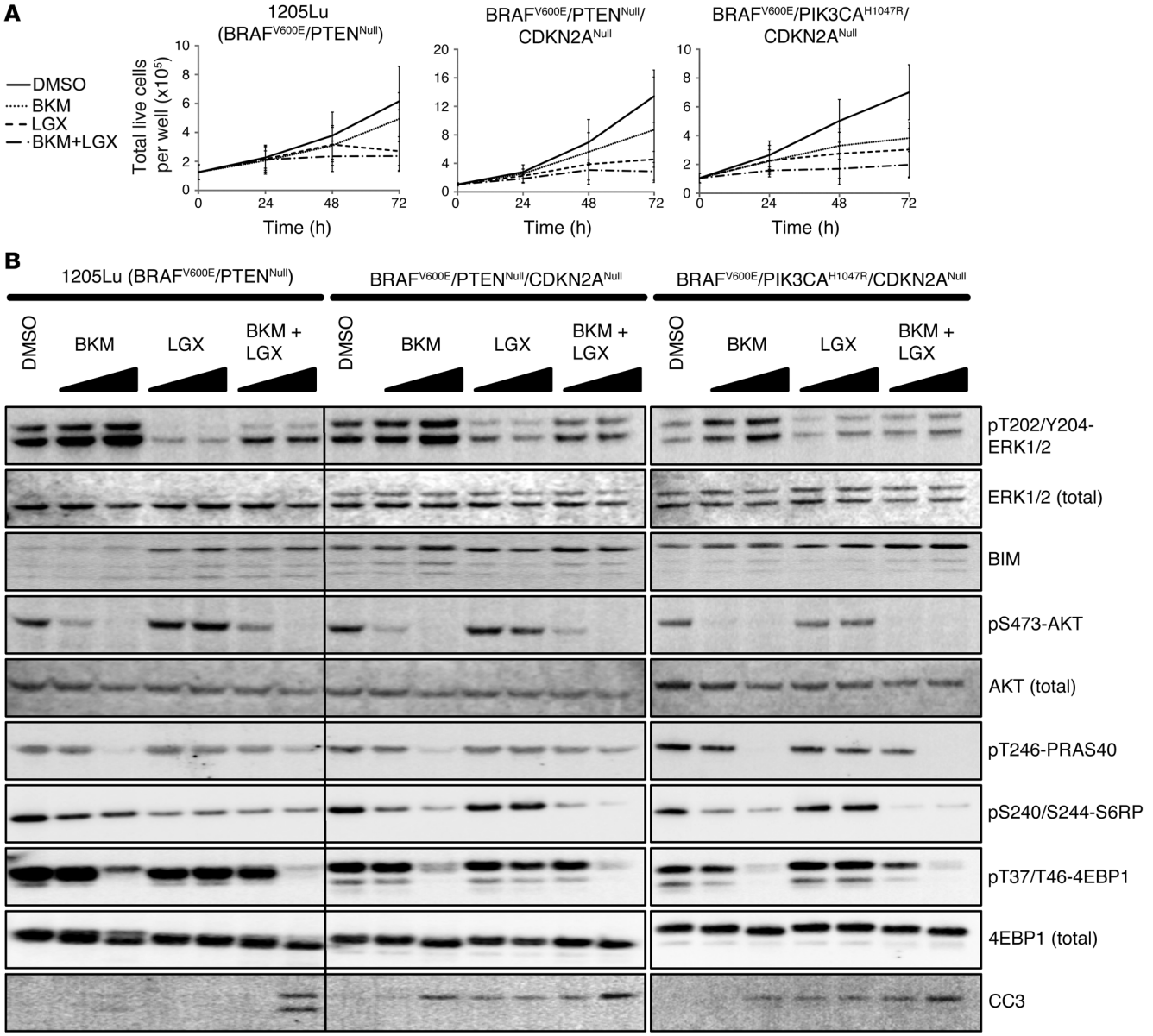

Figure 5

Treatment of melanoma-derived cell lines with a BRAF^{V600E}-specific inhibitor, LGX-818, is enhanced by combined PI3K inhibition using BKM-120. (**A**) Cells were grown in the presence of either 320 nM BKM-120 (dotted line), 80 nM LGX-818 (dashed line), both agents in combination (dot-and-dash line), or DMSO only (solid line), and counted every 24 hours for a total period of 72 hours. Total numbers of live cells per well are indicated, ± SD. (**B**) Cell lysates were obtained from all 3 cell lines treated with DMSO only, low-dose BKM-120 (320 nM), high-dose BKM-120 (5 μM), low-dose LGX-818 (80 nM), high-dose LGX-818 (1 μM), or combined low dose or combined high dose (320 nM BKM-120 + 80 nM LGX-818 and 5 μM BKM-120 + 1 μM LGX-818 respectively) for 24 hours as indicated. Lysates were probed with the antisera indicated.

of the study were assigned to have a +100% increase in tumor size. Those that displayed melanoma regression to a point at which melanomas could no longer be measured were determined to have a –100% change in tumor size. This analysis revealed that, while all mice on LGX-818 single-agent therapy displayed a striking regression of established melanomas, the majority of mice on combination LGX-818 plus BKM-120 therapy displayed enhanced antitumor responses, as observed by the clustering of these individual mice to the right of the plot (Figure 6D). Finally, after 50 days, we ceased drug dosing and evaluated whether possible remnant melanoma-initiating cells might promote regrowth of the tumors over the following 60–70 days. Melanomas in mice that had received single-agent LGX-818 regrew more rapidly compared with those that had received combination LGX-818 plus BKM-120 (Figure 6C), and this difference in tumor regrowth was statistically significant (Student's 1-tailed t test; $^*P < 0.01$).

Kaplan-Meier survival analysis of this experiment clearly indicated that single-agent BKM-120 provided no significant protection to BRAF^{V600E}/PTEN^{Null} melanoma–bearing mice from reaching their predetermined end point (Supplemental Figure 5E). In

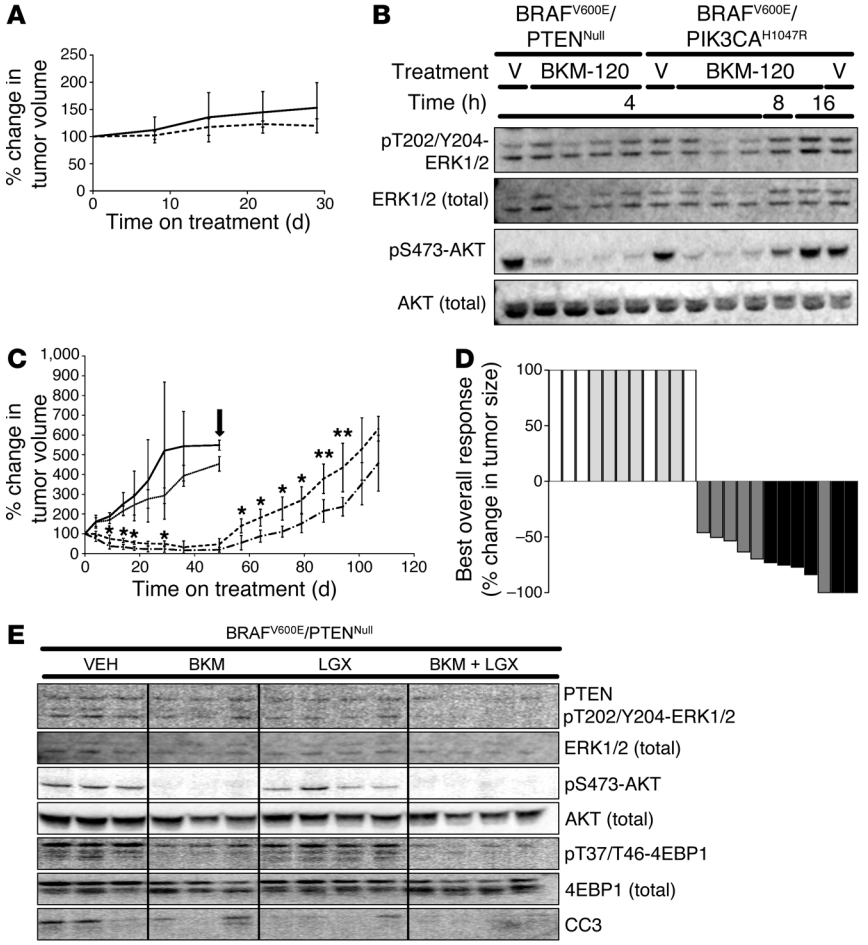

Figure 6
PI3K inhibition has modest antimelanoma therapeutic activity in vivo, but promotes regression of established tumors in response to $BRAF^{V600E}$ inhibition with LGX-818. (**A**) Growth of $BRAF^{V600E}$/$PIK3CA^{H1047R}$ melanomas in the absence (solid line) or presence of PI3K inhibitor BKM-120 (dashed line) was measured (displayed as percentage change in tumor volume ± SD). (**B**) Tumor lysates from vehicle- or BKM-120–treated $BRAF^{V600E}$/$PTEN^{Null}$ or $BRAF^{V600E}$/$PIK3CA^{H1047R}$ melanomas at 4–16 hours after dosing were probed with antisera against the various indicated proteins. (**C**) Established $BRAF^{V600E}$/$PTEN^{Null}$ melanomas (~45–60 days after initiation), were treated with vehicle (n = 5, solid line), BKM-120 (n = 6, dotted line), LGX-818 (n = 6, dashed line), or combined LGX-818/BKM-120 (n = 6, dot-dashed line). Tumors were measured weekly (displayed as percentage change in tumor volume ± SD). After 50 days, drug treatment ceased (indicated by arrow). Tumor measurement continued in mice that had received LGX-818 single-agent or combination therapy. $^{*}P < 0.01$; $^{**}P < 0.05$. (**D**) Best overall response of mice treated with vehicle (white bars), BKM-120 (light gray bars), LGX-818 (dark gray bars), or combination treatment (black bars). Mice with progressive disease over the course of the study were arbitrarily set to 100% change in tumor size. Mice bearing lesions that became unmeasurable during the course of treatment were determined to have a –100% change in tumor size. (**E**) Tumor lysates from $BRAF^{V600E}$/$PTEN^{Null}$ melanomas treated with vehicle, single-agent LGX-818, single-agent BKM-120, or LGX-818 plus BKM-120 in combination as indicated were probed with various antisera as indicated.

contrast, LGX-818 displayed a highly significant increase in mouse survival (Mantel-Cox log-rank test; $P < 0.01$). Finally, although the regrowth of melanomas treated with combined LGX-818 plus BKM-120 was slower than that of those treated with single-agent LGX-818, this did not translate into statistically significant enhanced survival of this cohort of mice.

To confirm on-target effects of the various therapeutic agents on cell signaling, melanoma cell lysates from mice receiving either control vehicle (VEH), BKM-120 (BKM), or LGX-818 (LGX) either alone or in combination (BKM + LGX) were analyzed by immunoblotting (Figure 6E). In BKM-120–treated mice, inhibition of pS473-AKT was readily evident. In contrast, only a modest reduction in pERK1/2 was observed in LGX-818–treated mice. However, this may reflect a combination of inhibition of pERK1/2 in $BRAF^{V600E}$/$PTEN^{Null}$ melanoma cells combined with activation of pERK1/2 in normal stromal cells that are found in these lesions. We also noted a more striking decrease of pERK1/2 in melanoma lysates from mice treated with combination LGX-818 plus BKM-120, although the reason for this is not clear. Consistent with the ability of $BRAF^{V600E}$ and PI3K signaling to cooperatively regulate mTorc1 signaling, we noted a more profound inhibition of 4E-BP1 phosphorylation in mice treated with LGX-818 plus BKM-120 compared with those treated with the single agents alone. In contrast with our findings in vitro, we observed no clear trend in the detected levels of CC3 following single-agent or combination treatment, suggesting that these treatment regimens may not induce caspase-mediated cell death in the in vivo setting.

Discussion

Malignant transformation of melanocytes is initiated and promoted by alterations in key cell signaling and cell-cycle pathways that ultimately cooperate for the maintenance of melanoma cells (1, 9, 10, 15, 54, 55). *BRAF* is the most frequently mutated protooncogene in melanoma and is sufficient to convert normal human or mouse melanocytes into benign melanocytic nevus cells (8–11, 56). However, through mechanisms that are gradually being unraveled, initiated $BRAF^{V600E}$-expressing melanocytes cease proliferation and enter into a state of cell-cycle arrest with features of senescence (12, 57, 58). However, mutational activation of *BRAF* in conjunction with silencing of tumor suppressors such as *PTEN* or *CDKN2A* or, as shown here, mutational activation of *PIK3CA*, which have no overt melanocytic phenotype on their own, allows rapid progression of $BRAF^{V600E}$-initiated melanocytes to malignant melanoma. Although not explicitly examined here, these alterations presumably facilitate bypass of senescence, consistent with observations of others (59). Moreover, we have made similar observations in mouse models of $BRAF^{V600E}$-induced lung or thyroid tumorigenesis (60, 61).

At the initiation of this research, silencing of *PTEN* was known to occur frequently in *BRAF*-mutated melanoma. In contrast,

mutational activation of *PIK3CA* was very rare in melanoma, despite high frequency *PIK3CA* mutations in other human cancers (17–19). More recently, however, mutational activation of PIK3CA has been reported in approximately 5% of melanoma specimens and cell lines (20, 62). Consistent with this, we report here that mutationally activated PIK3CA^{H1047R} can functionally cooperate with BRAF^{V600E} to promote melanomagenesis in a GEM model. Moreover, pharmacological intervention with BKM-120 indicates that class 1 PI3K activity is important for the cooperation of BRAF^{V600E} with PTEN silencing in both human and mouse melanoma. Although BRAF^{V600E}/PTEN^{Null} melanomas grew faster than their BRAF^{V600E}/PIK3CA^{H1047R} counterparts, the latter inevitably elicited end-stage disease. It remains possible that the observed differences in melanoma growth rate may reflect phosphatase-independent tumor suppressor activities of PTEN or differences in the tone of PI3K pathway activation (21–25). Recently, others demonstrated the ability of PIK3CA^{H1047R} expression to overcome BRAF^{V600E}-induced senescence in cultured melanocytes (59). Hence, the preponderance of PTEN silencing in melanoma may be due to mechanism(s) driving genetic or epigenetic alterations in melanomagenesis or to the timing of such alterations in disease progression. By the necessary use of the *Tyr::CreER^{T2}* transgene in the mouse, the genetic lesions in our models occurred concurrently. However, in human melanoma, events cooperating with BRAF^{V600E} in malignant progression are most likely temporally dissociated from the initiating event. Finally, human melanomas have been shown to harbor additional genetic/epigenetic abnormalities that contribute to malignant progression, which might influence the evolutionary trajectory of incipient melanoma cells toward PTEN silencing as opposed to PIK3CA activation.

Surprisingly, we noted that pharmacological inhibition of AKT using MK-2206 had little or no antitumor potency in preventing the growth of BRAF^{V600E}/PTEN^{Null} melanomas in our GEM model. In contrast, MK-2206 was highly effective against BRAF^{V600E}/PIK3CA^{H1047R} melanomas demonstrating an interesting tumor cell genotype–drug response relationship. Moreover, the efficacy of MK-2206 in preventing the growth of BRAF^{V600E}/PIK3CA^{H1047R} melanomas suggests that the agent's lack of potency against BRAF^{V600E}/PTEN^{Null} melanomas is not due to the dose or schedule of drug treatment. Moreover, these in vivo findings were mirrored when the effects of AKT inhibition on the growth of GEM model-derived cell lines or against the bona fide human 1205Lu BRAF^{V600E}/PTEN^{Null} melanoma cell line were assessed. Whereas AKT inhibition was highly effective at suppressing the growth of a mouse BRAF^{V600E}/PIK3CA^{H1047R} melanoma–derived cell line, this effect was much less profound in BRAF^{V600E}/PTEN^{Null} mouse or human melanoma cells. Indeed, these cells sustained their proliferation, albeit to a lesser extent compared with controls, even in the face of robust AKT inhibition with either of 2 structurally unrelated, mechanistically dissimilar agents. Furthermore, similar observations have been made in independent experiments using a wider panel of *BRAF*-mutated human melanoma cell lines regardless of their PTEN status (Jillian Silva and Martin McMahon, unpublished observations). Given the growth inhibitory effects of PI3K blockade, these data argue for a PI3K-dependent, AKT-independent mechanism of signal transmission in BRAF^{V600E}/PTEN^{Null} melanoma cells. Indeed, others have made similar observations of AKT-independent effects in cancers expressing mutationally activated PIK3CA (63). Although AKT is a protooncogene and clearly an important mediator of PI3K signaling in some circumstances, there are over 60 additional known PI3-lipid–regulated proteins including the TEC family of tyrosine kinases, the SGK family of serine/threonine kinases, guanine nucleotide exchange factors for RAS family GTPases, and more (38). Parsing out which of these is important for the cooperation of oncogenic BRAF^{V600E} with PTEN silencing may have important implications for understanding the inner workings of cancer cells including melanoma as well as for the future of combined chemotherapy for patients with genetically defined subsets of melanoma.

Finally, given the profound effects of PI3K inhibition in preventing melanomagenesis in vivo and melanoma cell growth in vitro, we tested this agent for efficacy in the more stringent therapeutic setting. In both our autochthonous GEM model and in 1205Lu xenografts, we were unable to detect significant therapeutic benefit to single-agent administration of BKM-120. This result may suggest that, despite its potent activity in the prevention setting, established melanomas are resistant to single-agent class 1 PI3K inhibition, perhaps through accumulation of additional mutations. Alternatively, the dosing regimen we have used, although sufficient to prevent the development of incipient melanomas, may not provide sufficient target coverage to have antitumor effects in the more rigorous therapy setting. However, when combined with LGX-818, a new and potent inhibitor of BRAF^{V600E}, we detected evidence of more rapid and profound melanoma regression compared with single-agent BRAF^{V600E} inhibition alone.

In conclusion, we report here that mutational activation of *PIK3CA* is sufficient to cooperate with BRAF^{V600E} expression to promote melanoma progression, in a manner similar to that seen following PTEN silencing. We also find that PI3K activity is necessary for melanoma growth in GEM models and that BRAF^{V600E}/PTEN^{Null} melanomas can develop independently of AKT activity. However, it remains to be seen whether the modest therapeutic benefit of combining class 1 PI3K inhibition with BRAF^{V600E} inhibition in GEM models will be sufficient to support clinical trials of these agents in patients with BRAF^{V600E}/PTEN^{Null}- or BRAF^{V600E}/PIK3CA^{H1047R}-driven melanomas.

Methods

Experimental animals. Mice were maintained on an outbred background and housed in a specified pathogen–free facility. Mice bearing the *Tyrosinase::CreER^{T2}* transgene (*Tyr::CreER^{T2}*), Cre-activated *BRaf* (*BRaf^{CA}*), or *Pik3ca* (*Pik3ca$^{Lat\text{-}1047R}$*) alleles or the Cre-inactivated *Pten* (*Pten$^{lox4\text{-}5}$*) or *Cdkn2a* (*Cdkn2a^{lox}*) alleles were intercrossed to generate experimental mice that were genotyped as previously described (32–35, 40). Melanocyte-specific Cre activity was induced in adult mice by topical application of 1 μl of 5 mM 4-HT (70% Z-isomer, in 100% Ethanol, Sigma-Aldrich) to shaved back skin. Melanoma growth was measured using calipers with tumor size estimated using the ellipsoid volume formula; $4/3\pi(\text{length}/2)(\text{width}/2)(\text{depth}/2)$. For xenograft studies, athymic nude female mice (Taconic Farms) were implanted bilaterally with 2.5×10^6 1205Lu human melanoma cells suspended in sterile PBS. Animals were euthanized when showing signs of ill health or when tumor volume exceeded 1000 mm^3, whichever occurred first.

At necropsy, tissues were fixed (Z-Fix; Anatech Ltd.) or snap frozen in liquid N_2. Fixed tissues were paraffin embedded, and sections were cut (5 μm thick) and stained using H&E or were used for immunostaining (see below). Protein lysates were generated from snap-frozen tumor samples by homogenization in RIPA buffer (50 mM Tris, 150 mM sodium chloride, 0.5 mM EDTA, 10 mM sodium fluoride 0.1% SDS, 0.5% sodium deoxycholate, 1% [v/v] NP-40) with added protease and phosphatase inhibitor cocktail (Halt; Pierce/Thermo Scientific). Protein concentrations were determined by BCA assay (Pierce/Thermo Scientific).

Primary antibodies for immunostaining were anti-tyrosinase (PEP7, gift of Vincent Hearing, NIH, Bethesda, Maryland, USA), anti-S100 (Clone 4C4.9; LabVision), and anti-Ki67 antigen (AbCam). Antigens were unmasked using boiling citrate buffer (Thermo Scientific). Primary antibodies were incubated overnight at 4°C. An Avidin-Biotin detection system was used to visualize primary antibody binding (Vectastain Elite ABC Kit; Vector Laboratories), employing DAB (DAB+ Kit; Dako).

Treatment of mice with pathway-targeted therapeutics. MK-2206 (obtained from Merck Pharmaceuticals) was prepared in 30% (v/v) Captisol (CyDex Pharmaceuticals) and administered at a dose of 480 mg/kg/wk. NVP-BKM-120 and LGX-818 (both obtained from Novartis Pharmaceuticals) were prepared in 0.5% (v/v) carboxymethylcellulose/0.5% (v/v) Tween-80 (Sigma-Aldrich) either as single agents or together and were administered at a dose of 30 mg/kg/d 6 days per week.

In tumor prevention studies, drug treatments commenced approximately 1 month after 4-HT–mediated induction of melanomagenesis and before tumors were readily measurable. Animals with approximately equal tumor sizes and sexes were assigned to receive either drug or vehicle control by oral gavage. Tumors were measured once per week, and at the end of the study, animals were euthanized 4 hours after a final dose of drug.

For therapy studies in autochthonous or xenografted tumors, tumors were grown until the mean tumor size of the cohort exceeded 500 mm^3. At this point, mice were assigned to receive treatment (prepared and administered as described above) or vehicle control by equally distributing mice between experimental groups based on their primary tumor size and their sex.

Melanoma cell culture, proliferation assays, and extraction. Growth medium for human and mouse melanoma cell lines was DME H-16 medium supplemented with 10% (v/v) fetal calf serum, 5 g/ml of insulin, L-glutamine, and penicillin (100 units/ml), and streptomycin (100 mg/ml).

Mouse melanoma cell lines were established from $BRAF^{V600E}$/$PTEN^{Null}$/$CDKN2A^{Null}$ or $BRAF^{V600E}$/$PIK3CA^{H1047R}$/$CDKN2A^{Null}$ tumors. Tumors were removed and kept in serum-free medium on ice before being microdissected to remove normal skin and blood vessels. Tumors were then cut into small pieces and incubated in Liberase TL (0.5 mg/ml in serum-free medium; Roche Applied Science) before being mechanically dissociated using a MediMachine (BD Biosciences). Cell suspensions were filtered (70 μm) before plating in growth medium (64, 65).

Cell proliferation was assessed by seeding 10^5 cells in the wells of a 12-well dish. Cells were treated with GSK2118436 (1 μM, provided by GlaxoSmithKline), PD3025901 (1 μM, Hansun International Trading Co.), SCH772984 (1 μM, provided by Merck Pharmaceuticals), GDC-0941 (5 μM, provided by Genentech), BKM-120 (5 μM), MK-2206 (5 μM, provided by Merck Pharmaceuticals), or GSK690603 (5 μM, provided by GlaxoSmithKline) for up to 6 days, with fresh medium and drugs applied at day 3. Cell numbers were determined using a Countess Automated Cell Counter (Life Technologies) using Trypan blue staining to quantify live cells. Data presented are representative of a minimum of 3 independent experiments. Cell pellets were collected in cold PBS containing 5 mM EDTA, lysed in RIPA buffer, and centrifuged at 18,000 *g* for 5 minutes at 4°C to generate a postnuclear supernatant for analysis by immunoblotting as described for tumor cell extracts above.

Immunoblotting. Primary antibodies for immunoblotting were as follows: ERK1/2 (total, no. 9107), phospho-ERK1/2 (pT202/pY204, no. 4370), AKT (total, no. 9272), phospho-AKT (pS473, no. 4060 or pT308, no. 2965), S6 ribosomal protein (S6RP) (total, no. 2317), phospho-S6RP (pS240/S244, no. 5364), phospho-PRAS40 (pT246, no. 2691), 4EBP1 (total, no. 9644), phospho-4EBP1 (pT37/pT46, no. 2855), PTEN (no. 9188), CC3 (D185, no. 9664) (all Cell Signaling Technology), BIM (no. 1036-1; Epitomics), and β-actin (clone AC-74; Sigma-Aldrich).

Using polyacrylamide Bis-Tris gels (Novex NuPage; Life Technologies), 50 μg of protein was separated and transferred to PVDF membrane (iBlot; Life Technologies). Membranes were blocked for 2 hours in Odyssey Blocking Buffer (LI-COR Biosciences) before application of primary antibody diluted in 1% (w/v) BSA (fraction V; MP Biomedical) in tris-buffered saline/0.1% (v/v) Tween-20. Membranes were incubated overnight at 4°C in primary antibody before detection using fluorescent goat anti-rabbit IRDye800 or anti-mouse IRDye680 secondary antibodies (LI-COR Biosciences) and visualized using an Odyssey Infrared Scanning System (LI-COR Biosciences).

Statistics. Survival analysis was performed using the Kaplan-Meier method and was performed using the SPSS analysis software package (version 20; IBM Inc.). Censored data points (where animals were removed from the study before reaching the defined end point) are indicated as tick-marks on survival curves. Statistical analysis for differences in survival distributions was performed using the Mantel-Cox log-rank test with $P < 0.01$ considered significant.

Student's 1-tailed *t* tests were employed to assess significant differences in tumor size in various mouse cohorts. $P < 0.01$ was considered significant.

Box-and-whisker plots were constructed to visualize the distribution of tumor sizes in treated versus untreated mouse cohorts. Plots were constructed such that the ends of whiskers indicate the maximum and minimum values of the data group, the upper and lower bounds of boxes indicate the upper (75th percentile) and lower (25th percentile) quartiles of the data, respectively, and the line intersecting the box indicates the median point of the data.

Study approval. Prior to commencement of this study, all animal procedures were reviewed and approved by the UCSF IACUC.

Acknowledgments

We thank all members of the McMahon lab for advice and guidance on this project, especially Jillian Silva for permission to cite unpublished research. We thank Vincent Hearing (NIH) for supplying antisera against mouse melanocyte proteins and Tim McCalmont, Boris Bastian, Scott Kogan (UCSF), and the Center for Genomic Pathology for histopathological evaluation of mouse melanomas. We thank Adil Daud (UCSF) and Antoni Ribas (UCLA) for stimulating discussions on melanoma therapy, Meenhard Herlyn (Wistar Institute) for providing melanoma cell lines, and Glenn Merlino (NCI) for critical advice on the generation of mouse melanoma cell lines. We thank our colleagues in various biotechnology and pharmaceutical companies for providing the following compounds and information on their use: Steven Townson, Heike Keilhack and Ahmed Samatar for MK-2206 and SCH772984 (Merck Pharmaceuticals); Emmanuelle di Tomaso, Janet Lyle, and Darrin Stuart for BKM-120 (Novartis); Leisa Johnson and Lori Freedman for GDC-0941 (Genentech); and Tona Gilmer and Kirin Patel for GSK2118436 (GlaxoSmithKline). We thank Byron Hann and the Helen Diller Family Comprehensive Cancer Center's Pre-clinical Therapeutics Core for advice on xenograft implantation and drug administration to mice. This research was supported by grants from the Melanoma Research Alliance (to M. McMahon) and from the NIH/NCI CA176839 (to M. McMahon) and CA112054 (to M.W. Bosenberg) and by project grants from the National Health and Medical Research Council of Australia to W.A. Phillips.

Received for publication March 1, 2013, and accepted in revised form September 3, 2013.

Address correspondence to: Martin McMahon, University of California San Francisco, Helen Diller Family Comprehensive

Cancer Center, MC-0128, 1450 Third Street, San Francisco, California 94158, USA. Phone: 415.502.5829; Fax: 415.502.3179; E-mail: mcmahon@cc.ucsf.edu.

Victoria Marsh Durban's present address is: European Cancer Stem Cell Research Institute, Cardiff University, Cardiff, United Kingdom.

1. Chin L, Merlino G, DePinho RA. Malignant melanoma: modern black plague and genetic black box. *Genes Dev*. 1998;12(22):3467–3481.
2. Jemal A, et al. Annual report to the nation on the status of cancer, 1975–2009, featuring the burden and trends in human papillomavirus (HPV)-associated cancers and HPV vaccination coverage levels. *J Natl Cancer Inst*. 2013;105(3):175–201.
3. Flaherty KT, et al. Inhibition of mutated, activated BRAF in metastatic melanoma. *N Engl J Med*. 2010; 363(9):809–819.
4. Flaherty KT, et al. Combined BRAF and MEK inhibition in melanoma with BRAF V600 mutations. *N Engl J Med*. 2012;367(18):1694–1703.
5. Davies H, et al. Mutations of the BRAF gene in human cancer. *Nature*. 2002;417(6892):949–954.
6. Pollock PM, et al. High frequency of BRAF mutations in nevi. *Nat Genet*. 2003;33(1):19–20.
7. Bennett DC. Human melanocyte senescence and melanoma susceptibility genes. *Oncogene*. 2003; 22(20):3063–3069.
8. Michaloglou C, et al. BRAFE600-associated senescence-like cell cycle arrest of human naevi. *Nature*. 2005;436(7051):720–724.
9. Dankort D, et al. BRAF(V600E) cooperates with PTEN loss to induce metastatic melanoma. *Nat Genet*. 2009;41(5):544–552.
10. Dhomen N, et al. Oncogenic Braf induces melanocyte senescence and melanoma in mice. *Cancer Cell*. 2009; 15(4):294–303.
11. Goel VK, et al. Melanocytic nevus-like hyperplasia and melanoma in transgenic BRAFV600E mice. *Oncogene*. 2009;28(23):2289–2298.
12. Peeper DS. Oncogene-induced senescence and melanoma: where do we stand? *Pigment Cell Melanoma Res*. 2011;24(6):1107–1111.
13. Goel VK, Lazar AJ, Warneke CL, Redston MS, Haluska FG. Examination of mutations in BRAF, NRAS, and PTEN in primary cutaneous melanoma. *J Invest Dermatol*. 2006;126(1):154–160.
14. Haluska FG, Tsao H, Wu H, Haluska FS, Lazar A, Goel V. Genetic alterations in signaling pathways in melanoma. *Clin Cancer Res*. 2006; 12(7 pt 2):2301s–2307s.
15. Whiteman DC, Pavan WJ, Bastian BC. The melanomas: a synthesis of epidemiological, clinical, histopathological, genetic, and biological aspects, supporting distinct subtypes, causal pathways, and cells of origin. *Pigment Cell Melanoma Res*. 2011;24(5):879–897.
16. Maehama T, Dixon JE. The tumor suppressor, PTEN/MMAC1, dephosphorylates the lipid second messenger, phosphatidylinositol 3,4,5-trisphosphate. *J Biol Chem*. 1998;273(22):13375–13378.
17. Campbell IG, et al. Mutation of the PIK3CA gene in ovarian and breast cancer. *Cancer Res*. 2004; 64(21):7678–7681.
18. Samuels Y, et al. High frequency of mutations of the PIK3CA gene in human cancers. *Science*. 2004; 304(5670):554.
19. Omholt K, Krockel D, Ringborg U, Hansson J. Mutations of PIK3CA are rare in cutaneous melanoma. *Melanoma Res*. 2006;16(2):197–200.
20. Hodis E, et al. A landscape of driver mutations in melanoma. *Cell*. 2012;150(2):251–263.
21. Shen WH, et al. Essential role for nuclear PTEN in maintaining chromosomal integrity. *Cell*. 2007; 128(1):157–170.
22. Song MS, et al. Nuclear PTEN regulates the APC-CDH1 tumor-suppressive complex in a phosphatase-independent manner. *Cell*. 2011;144(2):187–199.
23. Wu H, Goel V, Haluska FG. PTEN signaling pathways in melanoma. *Oncogene*. 2003; 22(20):3113–3122.
24. Li AG, Piluso LG, Cai X, Wei G, Sellers WR, Liu X. Mechanistic insights into maintenance of high p53 acetylation by PTEN. *Mol Cell*. 2006;23(4):575–587.
25. Rankin SL, Guy CS, Mearow KM. PTEN down-regulates p75NTR expression by decreasing DNA-binding activity of Sp1. *Biochem Biophys Res Commun*. 2009;379(3):721–725.
26. Held MA, Curley DP, Dankort D, McMahon M, Muthusamy V, Bosenberg MW. Characterization of melanoma cells capable of propagating tumors from a single cell. *Cancer Res*. 2010;70(1):388–397.
27. Damsky WE, et al. β-Catenin signaling controls metastasis in Braf-activated Pten-deficient melanomas. *Cancer Cell*. 2011;20(6):741–754.
28. Chen Z, et al. Discovery of LGX818: a potent, selective RAF kinase inhibitor for treatment of $BRAF^{V600E}$-positive melanoma. Presented at: 245th American Chemical Society National Meeting and Exposition; April 7–11, 2013; New Orleans, Lousiana, USA.
29. Drahl C. LGX818, made to fight melanoma. *Chem Engineer News*. 2013;91(16):14.
30. Ribas A, Flaherty KT. BRAF targeted therapy changes the treatment paradigm in melanoma. *Nat Rev Clin Oncol*. 2011;8(7):426–433.
31. Smalley KS, et al. Meeting report from the 2011 international melanoma congress, Tampa, Florida. *Pigment Cell Melanoma Res*. 2011;25(1):E1–E11.
32. Kinross KM, et al. An activating Pik3ca mutation coupled with Pten loss is sufficient to initiate ovarian tumorigenesis in mice. *J Clin Invest*. 2012; 122(2):553–557.
33. Trotman LC, et al. Pten dose dictates cancer progression in the prostate. *PLoS Biol*. 2003;1(3):E59.
34. Dankort D, Filenova E, Collado M, Serrano M, Jones K, McMahon M. A new mouse model to explore the initiation, progression, and therapy of BRAF(V600E)-induced lung tumors. *Genes Dev*. 2007; 21(4):379–384.
35. Bosenberg M, et al. Characterization of melanocyte-specific inducible Cre recombinase transgenic mice. *Genesis*. 2006;44(5):262–267.
36. Nogueira C, et al. Cooperative interactions of PTEN deficiency and RAS activation in melanoma metastasis. *Oncogene*. 2010;29(47):6222–6232.
37. Mason VL. American association for cancer research - 101st annual meeting — investigating new therapeutic candidates: part 2. *IDrugs*. 2010;13(6):360–362.
38. Stephens L, Hawkins P. Signalling via class IA PI3Ks. *Adv Enzyme Regul*. 2010;51(1):27–36.
39. Hirai H, et al. MK-2206, an allosteric Akt inhibitor, enhances antitumor efficacy by standard chemotherapeutic agents or molecular targeted drugs in vitro and in vivo. *Mol Cancer Ther*. 2010;9(7):1956–1967.
40. Aguirre AJ, et al. Activated Kras and Ink4a/Arf deficiency cooperate to produce metastatic pancreatic ductal adenocarcinoma. *Genes Dev*. 2003; 17(24):3112–3126.
41. Smalley KS, Haass NK, Brafford PA, Lioni M, Flaherty KT, Herlyn M. Multiple signaling pathways must be targeted to overcome drug resistance in cell lines derived from melanoma metastases. *Mol Cancer Ther*. 2006;5(5):1136–1144.
42. Haass NK, et al. The mitogen-activated protein/extracellular signal-regulated kinase kinase inhibitor AZD6244 (ARRY-142886) induces growth arrest in melanoma cells and tumor regression when combined with docetaxel. *Clin Cancer Res*. 2008; 14(1):230–239.
43. Solit DB, et al. BRAF mutation predicts sensitivity to MEK inhibition. *Nature*. 2006;439(7074):358–362.
44. Laquerre S, et al. Abstract B88: A selective Raf kinase inhibitor induces cell death and tumor regression of human cancer cell lines encoding $B\text{-}Raf^{V600E}$ mutation. Poster presented at: AACR-NCI-EORTC International Conference: Molecular Targets and Cancer Therapeutics; November 15–19, 2009 Boston, Massachusetts, USA; 2009; 8(12):B88.
45. Morris EJ, et al. Discovery of a novel ERK inhibitor with activity in models of acquired resistance to BRAF and MEK inhibitors. *Cancer Discov*. 2013; 3(7):742–750.
46. Folkes AJ, et al. The identification of 2-(1H-indazol-4-yl)-6-(4-methanesulfonyl-piperazin-1-ylmethyl)-4-morpholin-4-yl-thieno[3,2-d]pyrimidine (GDC-0941) as a potent, selective, orally bioavailable inhibitor of class I PI3 kinase for the treatment of cancer. *J Med Chem*. 2008;51(18):5522–5532.
47. Maira SM, et al. Identification and characterization of NVP-BKM120, an orally available pan-class I PI3-kinase inhibitor. *Mol Cancer Ther*. 2012; 11(2):317–328.
48. Heerding DA, et al. Identification of 4-(2-(4-amino-1,2,5-oxadiazol-3-yl)-1-ethyl-7-{[(3S)-3-piperidinylmethyl]oxy}-1H-imidazo[4,5-c]pyridin-4-yl)-2-methyl-3-butyn-2-ol (GSK690693), a novel inhibitor of AKT kinase. *J Med Chem*. 2008; 51(18):5663–5679.
49. Rhodes N, et al. Characterization of an Akt kinase inhibitor with potent pharmacodynamic and antitumor activity. *Cancer Res*. 2008;68(7):2366–2374.
50. Brachmann SM, et al. Characterization of the mechanism of action of the pan class I PI3K inhibitor NVP-BKM120 across a broad range of concentrations. *Mol Cancer Ther*. 2012; 11(8):1747–1757.
51. Cartlidge RA, et al. Oncogenic BRAF(V600E) inhibits BIM expression to promote melanoma cell survival. *Pigment Cell Melanoma Res*. 2008;21(5):534–544.
52. Chou TC, Talalay P. Quantitative analysis of dose-effect relationships: the combined effects of multiple drugs or enzyme inhibitors. *Adv Enzyme Regul*. 1984; 22:27–55.
53. Brachmann SM, et al. Characterization of the mechanism of action of the pan class I PI3K inhibitor NVP-BKM120 across a broad range of concentrations. *Mol Cancer Ther*. 2012;11(8):1747–1757.
54. Chin L, et al. Cooperative effects of INK4a and ras in melanoma susceptibility in vivo. *Genes Dev*. 1997; 11(21):2822–2834.
55. Gray-Schopfer VC, da Rocha Dias S, Marais R. The role of B-RAF in melanoma. *Cancer Metastasis Rev*. 2005; 24(1):165–183.
56. Pollock PM, et al. Melanoma mouse model implicates metabotropic glutamate signaling in melanocytic neoplasia. *Nat Genet*. 2003;34(1):108–112.
57. Mooi WJ, Peeper DS. Oncogene-induced cell senescence — halting on the road to cancer. *N Engl J Med*. 2006;355(10):1037–1046.
58. Kaplon J, et al. A key role for mitochondrial gatekeeper pyruvate dehydrogenase in oncogene-induced senescence. *Nature*. 2013;498(7452):109–112.
59. Vredeveld LC, et al. Abrogation of BRAFV600E-induced senescence by PI3K pathway activation contributes to melanomagenesis. *Genes Dev*. 2012; 26(10):1055–1069.
60. Charles RP, Iezza G, Amendola E, Dankort D, McMahon M. Mutationally activated BRAF(V600E) elicits papillary thyroid cancer in the adult mouse. *Cancer Res*. 2011;71(11):3863–3871.
61. Trejo CL, et al. Mutationally activated PIK3CAH1047R cooperates with BRAFV600E in lung cancer progression [published online

ahead of print September 9, 2013]. *Cancer Res*. doi:canres.0681.2013.
62. Kim JE, et al. Comparison of growth factor signalling pathway utilisation in cultured normal melanocytes and melanoma cell lines. *BMC Cancer*. 2012;12:141.
63. Vasudevan KM, et al. AKT-independent signaling downstream of oncogenic PIK3CA mutations in human cancer. *Cancer Cell*. 2009;16(1):21–32.
64. Zaidi MR, et al. Interferon-γ links ultraviolet radiation to melanomagenesis in mice. *Nature*. 2011;469(7331):548–553.
65. Wolnicka-Glubisz A, King W, Noonan FP. SCA-1+ cells with an adipocyte phenotype in neonatal mouse skin. *J Invest Dermatol*. 2005;125(2):383–385.